



## The Impingement Flow Study on The Temperature Profile Perforated Plate

Fathima Rehana Munas<sup>1,2</sup>, Nor Asikin Abu Kasim<sup>1</sup>, Yu Kok Hwa<sup>1</sup>, Wong Wei Cong<sup>1</sup>, Muzathik<sup>2</sup>, Mohd Azmi Ismail<sup>1,\*</sup>

<sup>1</sup> School of Mechanical Engineering, Universiti Sains Malaysia Engineering Campus, Penang, Malaysia

<sup>2</sup> Department of Mechanical Engineering, Faculty of Engineering, South Eastern University of Sri Lanka, University Park, Oluvil, #32360, Sri Lanka

### ARTICLE INFO

#### Article history:

Received 8 January 2022

Received in revised form 28 March 2022

Accepted 30 March 2022

Available online 18 April 2022

#### Keywords:

Perforated plate; impingement jet; hot air impingement; staggered hole; tandem hole

### ABSTRACT

This paper presents the impingement flow study on the temperature profile perforated plate. Icing is one of the most hazardous threats in aviation and this leads to unsafe flight conditions. Hence, thermal anti-icing is very much useful in aircraft to prevent ice accretion on the surface. On the other hand, the hotspot temperature of this technique might destroy the Aluminum-based Bias Acoustic Liner (BAL) plate. Thus, it is highly essential to study the hotspot temperature profile on the perforated plate. This study is concerned with a numerical study of the convective heat exchange between an impinging air jet at temperatures of 70 °C and a structured perforated surface using the Fluent tool. The model is designed in an Aluminium plate with the dimensions of 100 mm x 100 mm x 1mm containing 0.15 cm diameter perforated hole. In addition, the 0.25 cm diameter circular nozzle is maintained at a constant jet-to-target distance of 3.71 cm. In this sense, the standard  $k-\omega$  turbulence model jet equation is applied to this three-dimensional domain with periodic boundary conditions for the Reynolds numbers ranges from 2000–9000. The simulations are performed based on the gap between two holes and the hole configuration (tandem and staggered) at different jet velocities. The simulation results reveal that there is a rapid increment in heat transfer with Reynolds number and the maximum local Nusselt number decreases by seven and increases to 24 when the Reynolds number varies from 2508.17 to 8778.588 at the surface of the perforated plate. The findings of the hole arrangement on the perforated plate indicate that the tandem hole configuration without a center hole is highly recommended for bias acoustic liners than the staggered configuration. Since the tandem hole arrangement has higher dimensionless temperature, a thicker high temperature layer will be developed at the outer surface. Hence, this kind of perforated plate is more suitable to prevent ice accretion in aircraft applications.

## 1. Introduction

Icing is one of the most hazardous threats in aviation and the built-up of ice on the aerodynamic surfaces of the aircraft, such as the leading edges of the tail and the nacelle lip-skin surface will cause an unsafe flight condition [1,2]. Ice may also ingest into the engine which can damage the fan and

\* Corresponding author.

E-mail address: [azmi\\_meche@usm.my](mailto:azmi_meche@usm.my)

<https://doi.org/10.37934/arfmts.94.2.4760>

the compressor blade of the aircraft. Thus, the hot air anti-icing system is necessary for the aircraft to be protected from ice accumulation and this is most reliable and effective for safe aircraft journeys. Piccolo Tube Anti-Icing (PTAI) and Swirl Anti-Icing (SAI) are the two examples of anti-icing tools using a hot bleed air anti-icing system. PTAI is the most popular and effective anti-icing tool, however, it has low average heat transfer efficiency, produces a lot of hotspots along targeted surface and potentially create run-back ice accretion on the downstream of the nacelle lip, increasing aircraft noise [3,4].

This noise can be reduced by modifying the engine itself. However, in most cases, this can affect the engine's performance. The acoustic liners which consist solid face sheet, honeycomb, and perforated back sheet offer an additional way of reducing noise without affecting the performance of the engine [4]. Commonly this is installed on the inner wall surface of the nacelle inlet section in order to absorb the radiated acoustic energy and to reduce the noise from the engine and compressor. On the other hand, installing this noise abatement technique on the nacelle's leading edge due to the limited size of nose cowl zones. However, combining this acoustic liner and anti-icing on the leading edge of a nacelle may be ineffective at reducing forward-radiated noise and optimizing the thermal performance of the anti-icing system, as the acoustic liner's solid face sheet acts as an insulation barrier, preventing the heat required for anti-ice formation from being conducted [5].

Three sheets comprise the Acoustic Liner: a solid face sheet, a honeycomb back sheet, and a perforated back sheet [4]. As a result, a bias acoustic liner (BAL) shown in Figure 1 is placed in that limited area to compensate for the heat transfer to the nacelle lip cowl zone being non-uniform [6]. This BAL is made up of two porous plates: a face sheet and a back sheet, separated by a honeycomb channel. Rather than a solid face sheet, the perforated back sheet allows hot air from the anti-icing system to flow through and it is released to the nacelle lip-skin and nose-cowl regions very easily [7]. BAL also has wider and tuneable sound absorption due to various bias flow velocities through the perforated face plate. Further, this gives higher average absorption, higher heat transfer rate, and longer life cycle than AL [8-10].

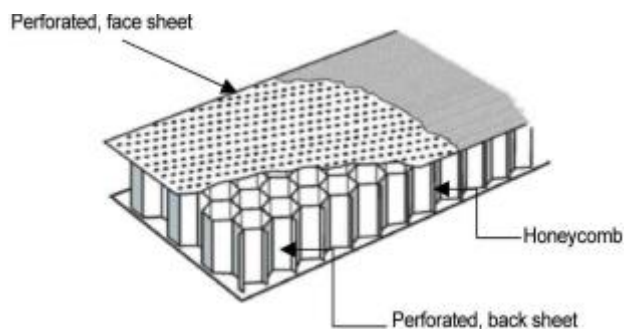


**Fig. 1.** Bias Acoustic Liners [7]

On the other hand, the hotspot temperature of anti-icing might destroy Bias Acoustic Liner surface, since Bias Acoustic Liner is fabricated by thin aluminium plate. Thus, it is highly essential to study the hotspot temperature profile on the perforated plate needs to be studied. However, there are limited research on the hotspot temperature profile of impingement hot air flow on the perforated plate at different holes arrangements and Reynolds number.

### 1.1 Impingement Jet Study

There are several researchers have conducted research experimentally as well as computationally to ascertain the impinging jet's heat transfer properties [11-15]. The impingement jet flow is

classified by three regions namely, free jet region, stagnation region and the wall jet region as shown in the Figure 2 [16,17]. The free jet region is defined as the zone within which the impingement plate has no effect flow. The velocity is predominantly axial and consistent along the jet centrelines. On the other hand, the flow is deflected away from its axial direction and into a radial direction in the stagnation region. The impact of increased heat transfer coefficients leads to the thinning of the boundary layer and an increase in turbulence intensity in this zone. In the wall jet zone, the velocity is mostly radial with the formation of a boundary layer along the radial direction [16].

In this configuration, the circular nozzle creates an air jet which is perpendicular to the impingement plate and this air jet is a kind of forced convection heat transfer resulting a turbulent regime near the stagnation point. Fundamentally, the turbulence in the jet flow is a function of the Reynolds number greater than 2000 [15,17].

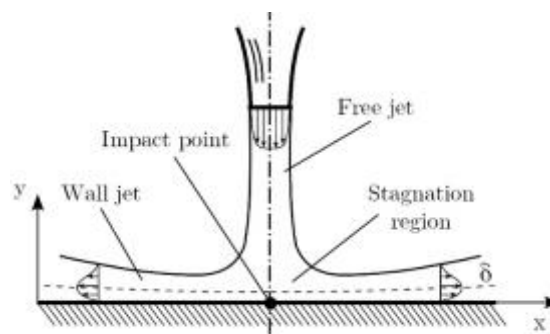


Fig. 2. Jet Impingement to plate [16]

### 1.2 CFD Study on Impingement Jet

Computational fluid dynamics (CFD) models were used by Singh *et al.*, [18] to investigate heat transfer from heated surfaces at various Reynolds numbers. They discovered that the Nusselt number and heat transfer coefficient are increasing with the Reynolds number. In this method, the heat transfer rate was increased by raising the jet stream's turbulence intensity, which increases the jet velocity. Extensive early research studies were carried out by Lee *et al.*, [19] on air jets impinging on perforated plates installed between an impinging jet nozzle and the target plate. Here, the studies were carried out with and without a perforated plate. In this case, it was discovered that the average Nusselt number in the stagnation zone was doubled when it was simulated with the perforated plate. It was shown that the Reynolds number is an essential parameter for investigating heat transfer distribution. Recent research studies reveal that simulating heat transfer in this turbulent flow arrangement is quite complicated. However, the numerical models used for these studies have a significant impact on the heat transfer predictions. The research on heat transfer performance of an impinging circular air jet using a numerical model was carried out by Alenezi [20]. In order to benchmark the experimental data, he developed seven different turbulence models in CFD Fluent to compare the accurate predictions among the models. Papadakis *et al.*, [21] carried out research to evaluate five various eddy-viscosity models for a single jet impinging on a flat surface. The findings revealed that the SST turbulence model produced the most accurate and consistent results. Further, the SST model constrained that the kinetic energy levels in the stagnation zone increases the sensitivity of heat transfer estimates. Research investigations were performed on multi-jet impingement cooling on a flat plate using a CFD technique investigated multi-jet impingement cooling on a flat plate using a CFD technique [22,24]. According to the findings of four different turbulence models, the SST model can make accurate flow and heat transfer characteristics at a

minimal computing cost. As per the results, the region below the nozzle has the lowest temperature with the increase of Reynolds number. There were three different turbulence models named as SST k- $\epsilon$  model, k- $\epsilon$  model, and the quadratic k-  $\epsilon$  model used to investigate heat transfer from a free turbulent slot jet to a heated surface [24]. The findings derived that the SST k-  $\epsilon$  models are much closer to the experimental findings.

## 2. Methodology

### 2.1 Design of the Model

A three-dimensional model consists of a nozzle inlet, air domain, and the perforated plate is designed in SolidWorks using hot air anti-icing characteristics as shown in Figure 3. Further, this model is designed with the dimensions of 100 mm x 100 mm x 1mm containing 0.15 cm diameter perforated hole. In addition, the 0.25 cm diameter circular nozzle is maintained at a constant jet-to-target distance of 3.71 cm. The distance between two holes in tandem and staggered configurations is maintained at 1 cm, 2 cm, 3 cm, and 4 cm respectively.

### 2.2 Theoretical Aspects

Though the air flow exiting the nozzle is predicted by measuring the Reynolds number of the flow, the Re for impingement jet is predicted as:

$$Re_{avg} = \frac{\rho_{avg} u_o D_h}{\mu} \quad (1)$$

where  $\mu$  is the dynamic viscosity,  $\rho_{avg}$  is the Average density of air, and  $D_h$  is the hydraulic diameter.

The average Nusselt number is used to study the rate of heat transfer from the hot jet to the perforated plate and it is calculated as:

$$Nu_{avg} = \frac{\bar{h}_{avg} D_h}{k} \quad (2)$$

where  $D_h$  is the hydraulic diameter, and k is the air thermal conductivity.

Since there is no heat energy specified in the Fluent, the heat transfer coefficient is calculated using heat flux.

$$h = \frac{q}{(T_{hotairavg} - T_{surfaceavg})} \quad (3)$$

where  $q$  is the convection heat transfer,  $T_{hotairavg}$  is the air temperature of the nozzle, and  $T_{surfaceavg}$  is the air temperature of the exhaust.

### 2.3 Numerical Simulation

The design was divided into 19 smaller bodies discretized independently to facilitate meshing and get the desired structured mesh. Boundary Meshes for three-dimensional surfaces have constructed the air container and plate using the edge sizing method to avoid excessive mesh elements and lengthy computation time.

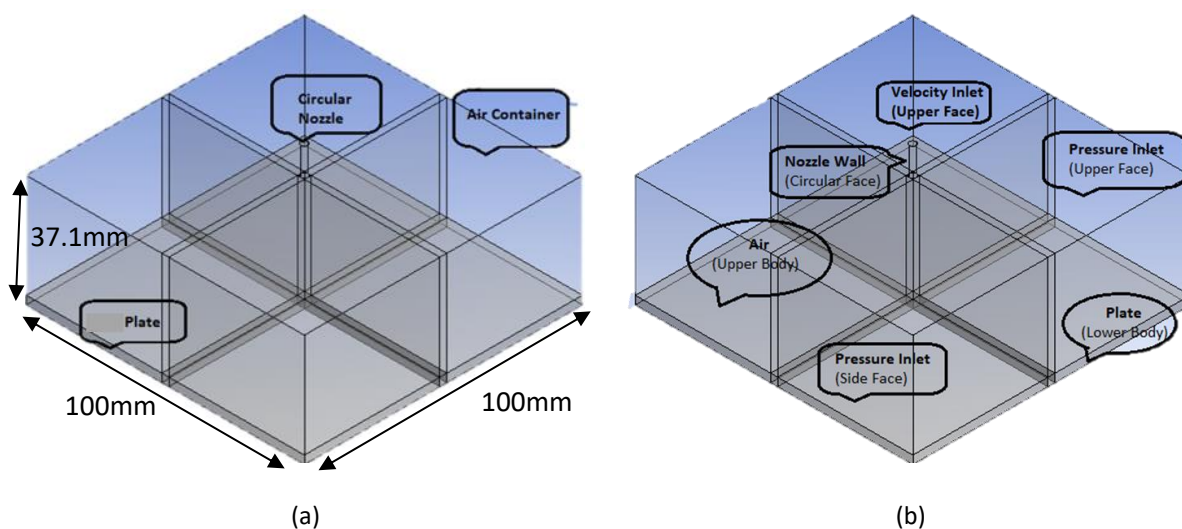
Though the flow is incompressible, the standard k- $\omega$  turbulence model jet equation is applied to this three-dimensional domain with periodic boundary conditions for the Reynolds numbers ranges from 2000–9000. The simulations are performed for eight different hole configurations on both tandems and staggered at 11 different jet velocities. The material selected for the plate is Aluminium.

Table 1 lists the computational boundary conditions for each material, along with their kinds and values for the effect of applied velocity and temperature. The pressure field was evaluated using the pressure-velocity coupling method (SIMPLE) (Semi Implicit Method for Pressure-Linked Equations). The turbulent kinetic energy and turbulent dissipation rate equations are solved using a first-order upwind discretization scheme. Then, the momentum, energy, and density equations are solved using a second-order upwind discretization scheme. When the energy equations reach a value of  $10^{-3}$ , the solutions are converged. The outcomes of the numerical simulations were compared to those acquired experimentally. Though there is no correlation between the Nusselt number and the Reynolds number for impingement jets on perforated plates, the correlation between the average Nusselt number and the Reynolds number for impingement on a flat plate is used. The same simulation setup is also used for validation. Thus, the average Nusselt number at the stagnation region for different velocities is simulated.

**Table 1**

The selection of boundaries according to conditions and values on the perforated plate

Boundary Conditions	Position	Value
Pressure Outlet	Side face of air container	Temperature: 27°C
Pressure Inlet	The upper face of the air container	Temperature: 27°C
Velocity Inlet	The upper face of the nozzle	Velocity magnitude: Eleven air velocities varied from 20 m/s to 70 m/s with an increment of 5 m/s Temperature: 70°C



**Fig. 3.** Isometric View of (a) jet impinges to plate system (b) boundary condition of Hot air impingement

### 3. Results and Discussion

#### 3.1 Validation of the Numerical Procedure

The simulation results obtained for the average Nusselt number at the stagnation region for different velocities were compared with the correlation made by Alenezi [20]. Figure 4 shows a comparison between the Nusselt number from simulation and the Nusselt number from correlation.

$$Nu_{avg} = 0.04592 \times Re^{0.6994} \quad (4)$$

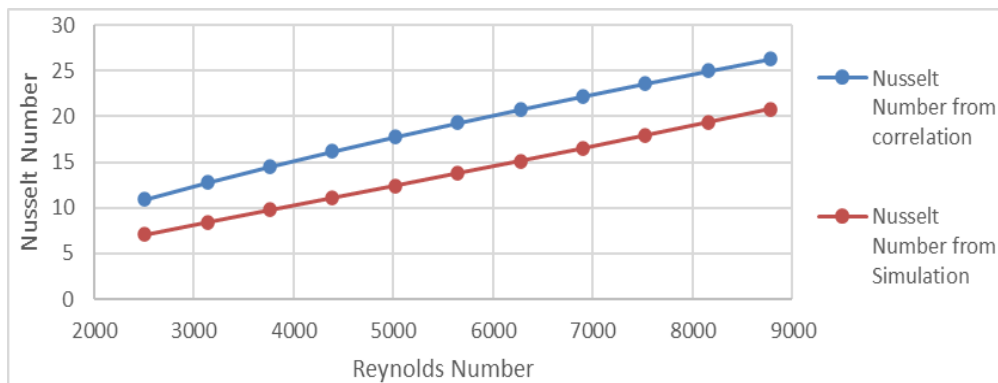


**Fig. 4.** Graph of Nusselt number against Reynolds number for correlation and simulation

The result discrepancy between the present study and empirical correlation happen because of the present model uses perforated plate and empirical correlation uses to predict thermal characteristic of flat plate. Besides, the thermal material properties, for example, thermal conductivity, and air flow characteristics i.e., air viscosity, air density, air thermal conductivity, and turbulent intensity of present work slightly different with empirical correlation.

#### 3.2 Impingement Flow Pattern on Perforated Plate

Since plotting the effect of velocity profile and the temperature profile for the impingement flow on the perforated plate is highly essential, these were obtained from simulation. The velocity profile of a 1 cm of tandem and staggered configurations moving at 70 m/s in the y-z plane with a hole in the center of the perforated plate exemplifies the hole configuration as shown in Figure 5(a) and Figure 5(b). According to the figures, a portion of the flow passes directly through the hole and escapes to another air domain with a hole in the center. On the other hand, a very less amount of flow expands radially.

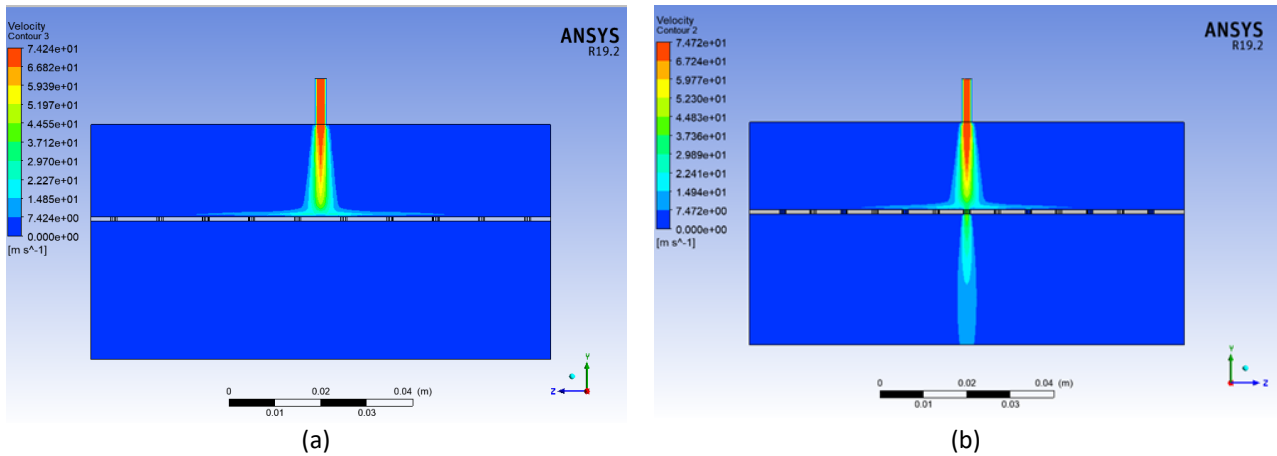


**Fig. 5.** (a) Velocity profile of 1 cm under 70 m/s in the y-z plane on a tandem perforated plate, (b) Velocity profile of 1 cm under 70 m/s in y-z plane on a staggered plate arrangement

### 3.3 Temperature Distribution on The Surface of a Perforated Plate under Different Average Reynolds Number

Though the dimensionless temperature is a key factor to evaluate the performance of each model analyzing the dimensionless temperature distribution on the surface of the perforated plate for various Reynolds Numbers is vital in this study. Thus, Figure 6 and Figure 7 show the dimensionless temperature distribution on the surface of the perforated plate for a 1 cm tandem arrangement under different Reynolds numbers along the x-axis and z-axis. According to the figures, the dimensionless temperature is steadily increasing in the range of 0.02 to 0.04 when the Reynolds number is slowly increasing from low values to high values.

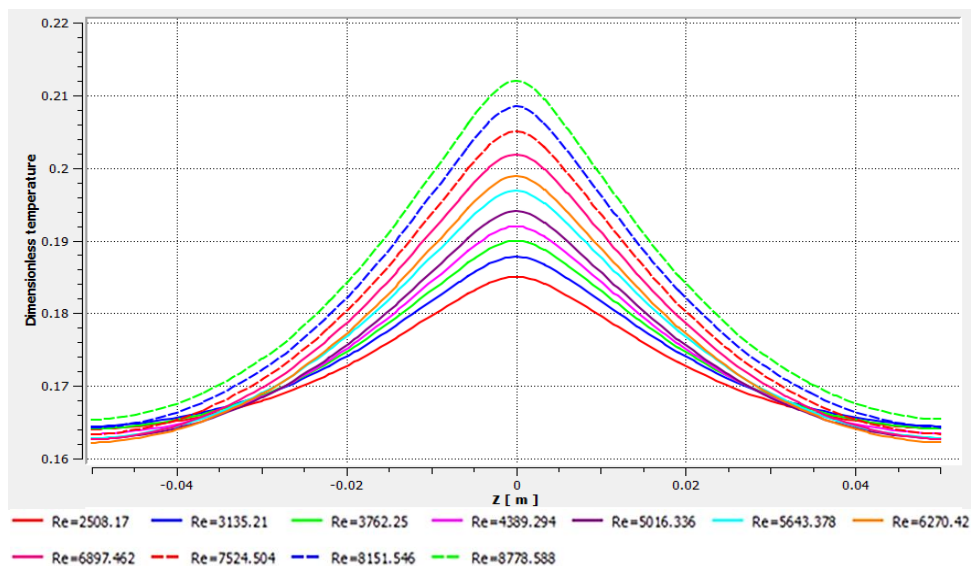


**Fig. 6.** Dimensionless temperature distribution of 1 cm tandem perforated plate for different Reynolds number along x-axis

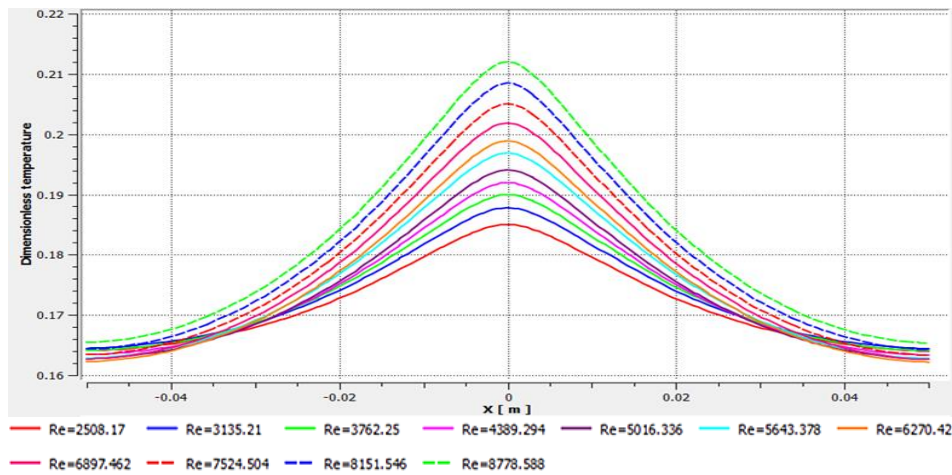


**Fig. 7.** Dimensionless temperature distribution of 1 cm tandem perforated plate for different Reynolds number along the z-axis

However, the increase in Reynolds number only provides a slight effect on the plate's temperature when the radial distance reached 2.4 cm. This is because the heat may not transfer from the jet to the perforated plate. Hence, the dimensionless temperature of the perforated plate increased with the increase of Reynolds number, given the radial distance of the plate is within the effective impingement area.

### 3.4 The Relationship between Reynolds Number and Nusselt Number to the Hot Air Impingement Study

Commonly, the local Nusselt number is used to evaluate the performance of the impingement jet on the perforated plate. Though the Nusselt number shows the ratio of convective over conductive heat transfer, which can better represent the heat transfer from the jet to the perforated plate. Therefore, a higher Nusselt number indicates the higher convective heat transfer for the impingement jet.

Plotting the variation of Nusselt number with the radial distance over nozzle diameter,  $r/D$  ratio is also very much useful. Hence, it is plotted in Figure 8 and it reveals that the Nusselt number is decreased exponentially as the radial distance over nozzle diameter,  $r/D$  ratio is increased. When the Reynolds number is increased, the Nusselt number is also increased. This is due to the lowest impingement jet velocity of 20 m/s has a Reynolds number of 2508.17, which is already turbulent. Any further increase in Reynolds number only increases the turbulence intensity but does not change the flow state.

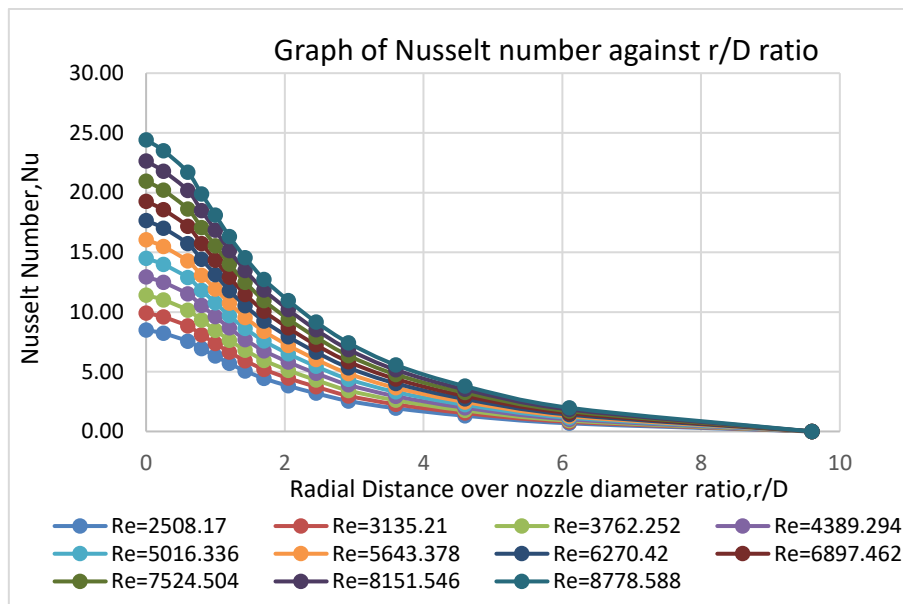


**Fig. 8.** Graph of Nusselt number against r/D ratio

### 3.5 The Effect of Holes Arrangement (Tandem and Staggered) on the Temperature Distribution of Perforated Plate in Impingement Flow Study.

The dimensionless temperature distribution for the surface of the perforated plate for different hole arrangements is studied to determine the suitable hole arrangement for bias acoustic liner to prevent the ice accretion on the surface of the aircraft.

The dimensionless temperature distribution for different hole arrangements of the perforated plate under low Reynolds number along the x-axis and z-axis are shown by Figure 9 and Figure 10 respectively. Since the hot air from the piccolo tube has a very high velocity, the temperature for different hole arrangements under high Reynolds number are plotted to study the dimensionless temperature distribution under high Reynolds number.

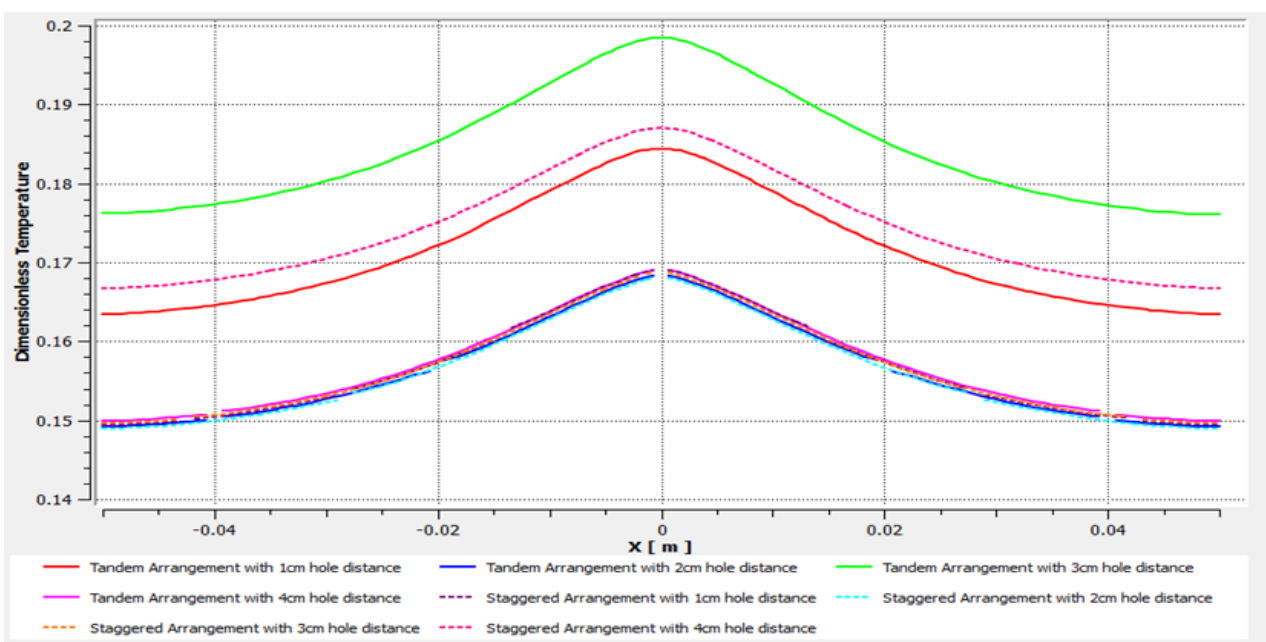


**Fig. 9.** Dimensionless temperature distribution of perforated plate for different hole arrangement under low Reynolds number along x-axis

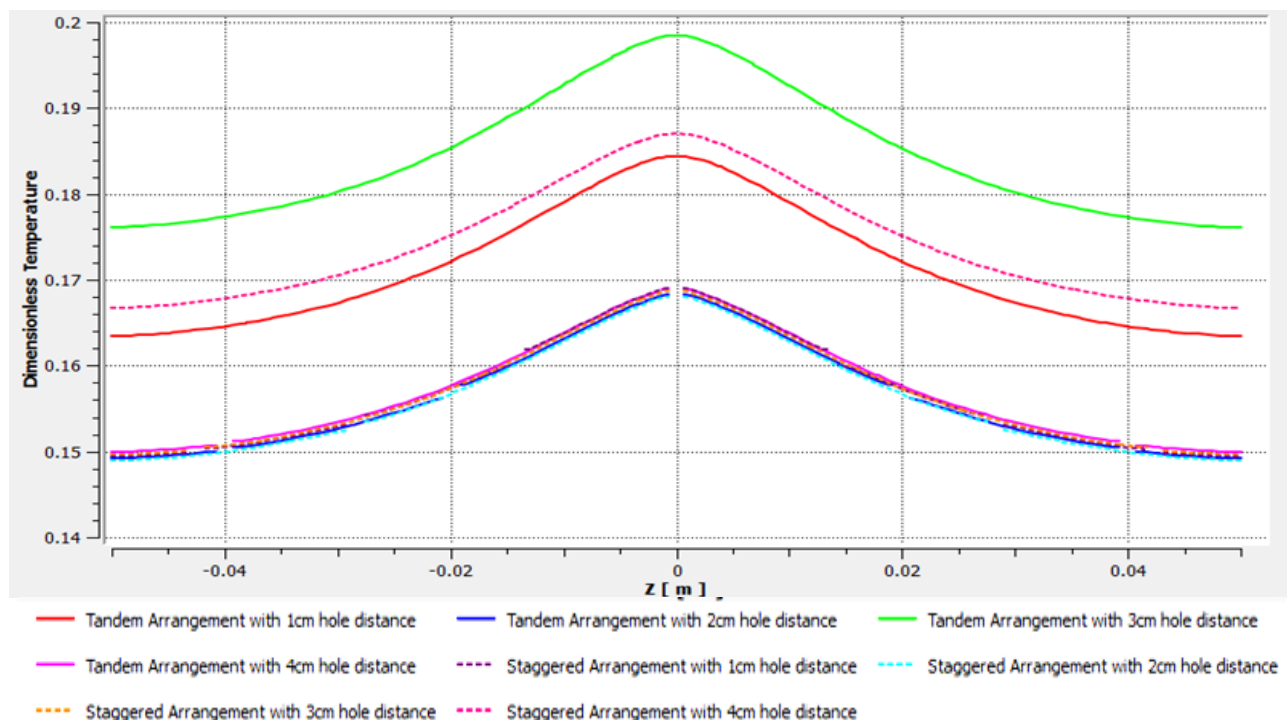


**Fig. 10.** Dimensionless temperature distribution of inner surface of perforated plate for different hole arrangement under low Reynolds number along z-axis

The temperature distribution of perforated plate for different hole arrangement under high Reynolds number along x-axis and z-axis are illustrated by Figure 11 and Figure 12 respectively. As per these figures, the 3 cm tandem arrangement shows the highest dimensional temperature of 0.198. On the other hand, the 4 cm staggered arrangement and 1 cm tandem arrangement have dimensionless temperatures of 0.186 and 0.184, respectively. Further, the dimensionless temperature is similar for other hole configurations as well. This is due to the 1 cm and 3 cm tandem arrangement and the 4 cm staggered arrangement does not have a hole at the center of the perforated plate, so the jet can directly impinge on the plate. but for other arrangements, a portion of the hot air is passed through the center hole when the jet impinged on the surface results in the heat transfer from the jet to the perforated plate is nearly the same.

At high Reynolds number, the difference between the dimensionless temperatures of 1 cm tandem arrangement, 3 cm tandem arrangement, and the 4 cm staggered arrangement become lesser, which only have differences in dimensionless temperature of 0.06. On the other hand, the velocity of the jet is lower at a low Reynolds number.

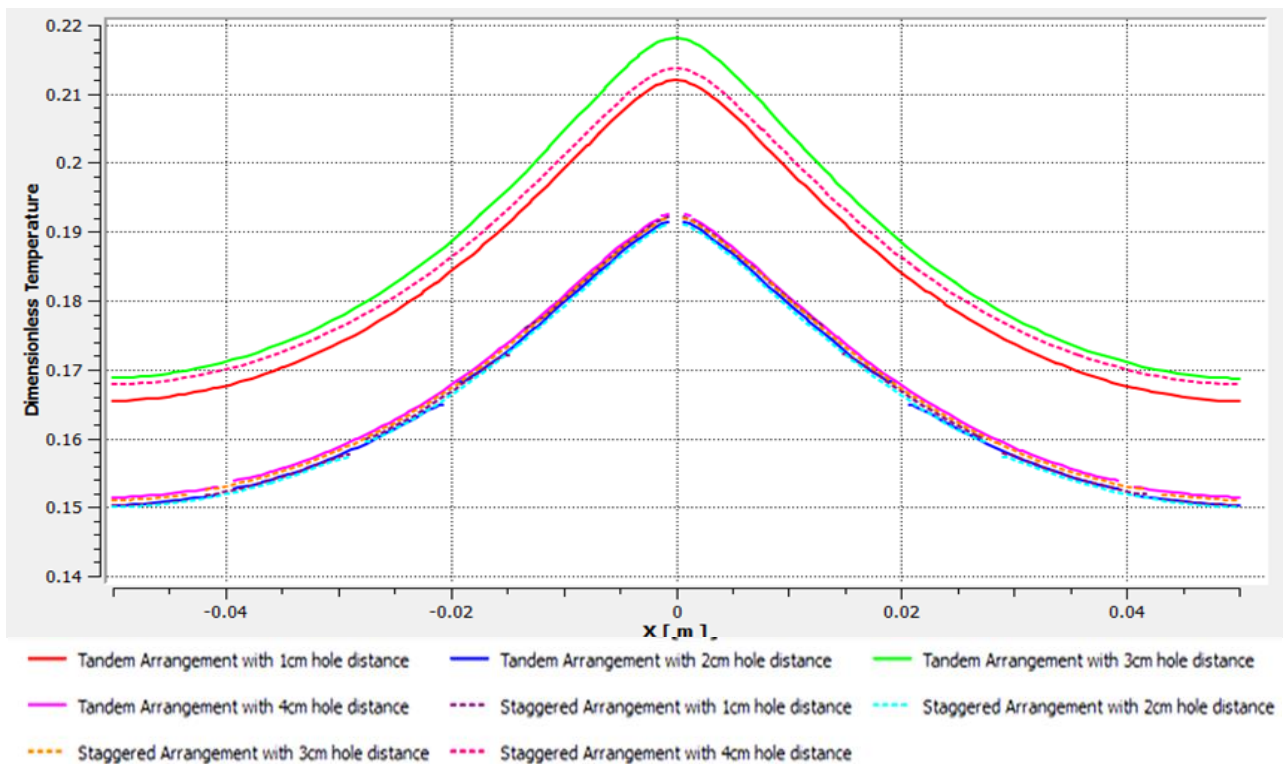


**Fig. 11.** Temperature distribution of perforated plate for different hole arrangement under high Reynolds number along x-axis

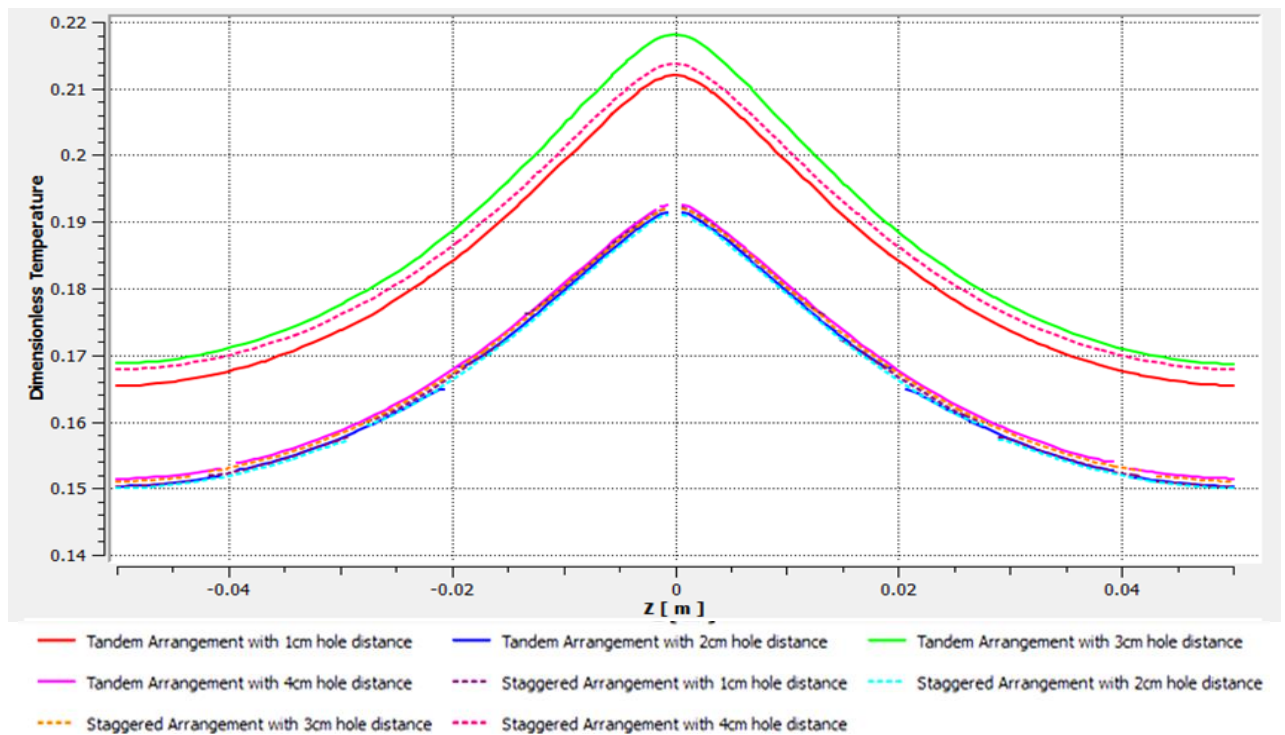


**Fig. 12.** Temperature distribution of perforated plate for different hole arrangement under high Reynolds number along the z-axis

### 3.5.1 Nusselt number of perforated plates for different hole arrangement

Since the Nusselt number is also one of the key parameters to analyze the temperature profile, the variation of the Nusselt number with  $r/D$  is obtained as shown in Figure 13(a) and Figure 13(b). These figures illustrate that the Nusselt number has an exponential decrement when the radial distance over nozzle diameter ratio,  $r/D$  increased. On the other hand, the Nusselt number for 3 cm tandem arrangement is higher under low Reynolds number and higher than other arrangements under high Reynolds number.

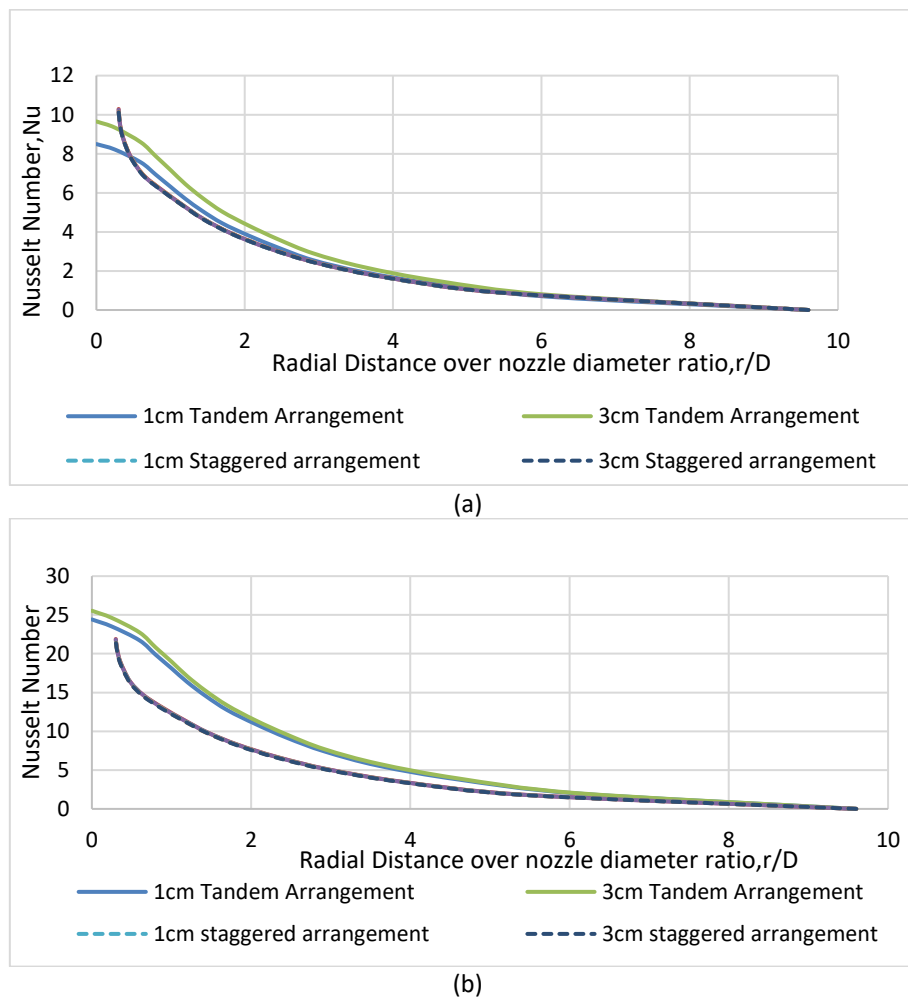


**Fig. 13.** (a) Graph of Nusselt number against  $r/D$  for different hole arrangement under low Nusselt number, (b) Graph of Nusselt Number against  $r/D$  for different hole arrangement under high Nusselt Number

## 4. Conclusions

The impingement hot air flow on perforated plates with various hole configurations is simulated using computational fluid dynamics for a range of Reynolds numbers. The simulation results reveal that there is an increase in dimensionless temperature of the perforated plates with the Reynolds number of the flows. The increment of this dimensionless temperature varying from 0.02 to 0.04 when the Reynolds number varying from low value to highest.

Comparing the results, the tandem hole configuration is more suitable for bias acoustic liners than the staggered hole configuration. In this regard, the difference in dimensionless temperature

between the 3 cm tandem hole configuration and the 4 cm staggered hole configuration is 0.1 and 0.4 for low and high Reynolds numbers. This temperature difference might be due to the staggered hole configuration that increases the hole distance in the streamwise and spanwise direction, affecting the flow mixing effects.

Considering the temperature profile developed after the jet impingement and the temperature distribution of the perforated plate for different hole arrangements, tandem hole configuration without a center hole is highly recommended. Further, the tandem hole configuration has a higher dimensionless temperature. Hence, a thicker high-temperature layer will be developed at the outer surface in order to make it more suitable for preventing ice accretion.

### Acknowledgment

This research was funded by a fundamental research grant scheme from Ministry of Higher Education of Malaysia (FRGS/1/2018/TK09/USM/03/3).

### References

- [1] Authority, Civil Aviation. "Aircraft icing handbook." *Safety Education and Publishing Unit: New Zealand* 2 (2000).
- [2] Rodríguez, Alonso Oscar Zamora. "Numerical investigation of a wing hot air ice protection system." *PhD diss., Wichita State University*, 2009.
- [3] Ismail, M. A., S. H. Mohammad Firdaus, S. Soid, M. Khalil, and H. Yusoff. "Numerical Investigation on Uniformity of Heat Distribution of Swirl Anti-Icing System." *Indian Journal of Science and Technology* 8, no. 30 (2015). <https://doi.org/10.17485/ijst/2015/v8i30/87312>
- [4] Ismail, Mohd Azmi bin. "Enhancement of heat transfer performance on nacelle lip-skin for swirl anti-icing." *PhD diss., Kingston University*, 2014.
- [5] Legendre, C., and L. M. B. C. Campos. "On sound absorption by an acoustic liner with bias flow." *29th Congress of the International Council of the Aeronautical Sciences* (2014): 1-12.
- [6] Ismail, Mohd Azmi, and Jian Wang. "Effect of nozzle rotation angles and sizes on thermal characteristic of swirl anti-icing." *Journal of Mechanical Science and Technology* 32, no. 9 (2018): 4485-4493. <https://doi.org/10.1007/s12206-018-0845-x>
- [7] Khai, Lee Chern, Mohd Azmi Ismail, Qummare Azam, and Nurul Musfirah Mazlan. "Experimental study on aerodynamic performance of nacelle lip-skin bias flow." *Journal of Mechanical Science and Technology* 34, no. 4 (2020): 1613-1621. <https://doi.org/10.1007/s12206-020-0323-0>
- [8] Ma, XuQiang, and ZhengTao Su. "Development of acoustic liner in aero engine: a review." *Science China Technological Sciences* 63, no. 12 (2020): 2491-2504. <https://doi.org/10.1007/s11431-019-1501-3>
- [9] Ives, Anthony O., Jian Wang, Srinivasan Raghunathan, and Patrick Sloan. "Heat transfer through a single hole bias flow acoustic liner." *Journal of Thermophysics and Heat Transfer* 25, no. 3 (2011): 409-423. <https://doi.org/10.2514/1.T3637>
- [10] Ibrahim, Thamir K., Marwah N. Mohammed, Mohammed Kamil Mohammed, G. Najafi, Nor Azwadi Che Sidik, Firdaus Basrawi, Ahmed N. Abdalla, and S. S. Hoseini. "Experimental study on the effect of perforations shapes on vertical heated fins performance under forced convection heat transfer." *International Journal of Heat and Mass Transfer* 118 (2018): 832-846. <https://doi.org/10.1016/j.ijheatmasstransfer.2017.11.047>
- [11] Nasif, G., R. M. Barron, and R. Balachandar. "Simulation of jet impingement heat transfer onto a moving disc." *International Journal of Heat and Mass Transfer* 80 (2015): 539-550. <https://doi.org/10.1016/j.ijheatmasstransfer.2014.09.036>
- [12] Nasif, Ghassan Gus. "CFD Simulation of Oil Jets with Application to Piston Cooling." *PhD diss., University of Windsor*, 2014.
- [13] Haidar, Chadia, Rachid Boutarfa, and Souad Harmand. "Numerical and Experimental Study of Convective Heat Exchanges on a Rotating Disk with an Eccentric Impinging Jet." *Journal of Advanced Research in Fluid Mechanics and Thermal Sciences* 57, no. 2 (2019): 208-215. <https://doi.org/10.1115/1.4044207>
- [14] Aroonrujiphan, Chattawat, and Chayut Nuntadusit. "Flow and Heat Transfer Characteristics of Impinging Bubbly Jet." *Journal of Advanced Research in Fluid Mechanics and Thermal Sciences* 74, no. 1 (2020): 68-80. <https://doi.org/10.37934/arfmts.74.1.6880>
- [15] Nasif, Ghassan, and Yasser El-Okda. "Conjugate Effect on the Thermal Characteristics of Air Impinging Jet." *CFD Letters* 13, no. 10 (2021): 25-35. <https://doi.org/10.37934/cfdl.13.10.2535>

- [16] Simionescu, Ștefan-Mugur, and Corneliu Bălan. "CFD study on convective heat exchange between impinging gas jets and solid surfaces." *Energy Procedia* 85 (2016): 481-488. <https://doi.org/10.1016/j.egypro.2015.12.231>
- [17] Mauri, Roberto. "Free Convection." In *Transport Phenomena in Multiphase Flows*, pp. 321-338. Springer, Cham, 2015. [https://doi.org/10.1007/978-3-319-15793-1\\_19](https://doi.org/10.1007/978-3-319-15793-1_19)
- [18] Singh, Jaspreet, Rakesh Kumar, and Parampreet Singh. "CFD Analysis of Investigation of Heat Transfer Using Single Swirling Jet Air Impingement with Twisted Tapes." *International Advanced Research Journal in Science, Engineering and Technology* 3, no. 6 (2016): 171-175. <https://doi.org/10.17148/IARJSET.2016.3633>
- [19] Lee, Dae Hee, Young Min Lee, Yun Taek Kim, S. Y. Wong, and Young Suk Chung. "Heat transfer enhancement by the perforated plate installed between an impinging jet and the target plate." *International Journal of Heat and Mass Transfer* 45, no. 1 (2002): 213-217. [https://doi.org/10.1016/S0017-9310\(01\)00134-X](https://doi.org/10.1016/S0017-9310(01)00134-X)
- [20] Alenezi, Abdulrahman. "Heat removal in high pressure turbine seal segments." *PhD diss., Cranfield University*, 2017.
- [21] Papadakis, Michael, M. Breer, N. Craig, and X. Liu. *Experimental water droplet impingement data on airfoils, simulated ice shapes, an engine inlet and a finite wing*. No. NAS 1.26: 4636. 1994.
- [22] Chandramohan, Palaniappan, S. N. Murugesan, and S. Arivazhagan. "Heat transfer analysis of flat plate subjected to multi-jet air impingement using principal component analysis and computational technique." *Journal of Applied Fluid Mechanics* 10, no. 1 (2017): 293-306. <https://doi.org/10.18869/acadpub.jafm.73.238.26337>
- [23] Chougule, N. K., G. V. Parishwad, P. R. Gore, S. Pagnis, and S. N. Sapali. "CFD analysis of multi-jet air impingement on flat plate." In *Proceedings of the World Congress on Engineering*, vol. 3, pp. 2078-0958. 2011.
- [24] Pawar, Shashikant, and Devendra Kumar Patel. "Performance analysis of different turbulence models in impinging jet cooling." *International Journal of Modern Physics C* 31, no. 04 (2020): 2050051. <https://doi.org/10.1142/S0129183120500515>